

# Stereo with Mirrors\*

Sameer A. Nene and Shree K. Nayar

Department of Computer Science  
Columbia University  
New York, NY 10027

## Abstract

*In this paper, we propose the use of mirrors and a single camera for computational stereo. When compared to conventional stereo systems that use two cameras, our method has a number of significant advantages such as wide field of view, single viewpoint projection, identical camera parameters and ease of calibration. We propose four stereo systems that use a single camera pointed towards planar, ellipsoidal, hyperboloidal, and paraboloidal mirrors. In each case, we present a derivation of the epipolar constraints. Next, we attempt to understand what can be seen by each system and formalize the notion of field of view. We conclude with two experiments to obtain 3-D structure. In the first we use a pair of planar mirrors, and in the second a pair of paraboloidal mirrors. The results of our experiments demonstrate the viability of stereo using mirrors.*

## 1 Introduction

Researchers have in the past looked at stereo techniques that attempt to obtain depth from omnidirectional data constructed from dioptric (purely lens based) imaging systems. Ishiguro *et al.* [6], and more recently Kang and Szeliski [7], have used panoramic cylindrical mosaics to compute depth and obtain a 3-D reconstruction of the scene. An image based rendering technique without explicit 3-D reconstruction uses a pair of cylindrical image mosaics [8]. In all these cases, omnidirectional data was obtained by first acquiring images by rotating or simply moving a conventional camera, and then projecting and mosaicing these images on a cylindrical surface. Such techniques need manual intervention, mechanical gadgetry, and a large amount of computation. Hence they are slow and cumbersome to adopt. However, they do have the advantage that the acquired data, and subsequently, the depth that is computed is of high resolution.

Nayar [11] suggested a wide field of view (FOV) stereo system that consisted of a conventional camera

pointed at two specular spheres (“Sphere”). Such an optical system, consisting of refracting and reflecting elements is called a *catadioptric system* [5]. He showed that establishing correspondence between the images of the scene reflected off the two spheres makes it possible to triangulate and compute depth. In [12], Nayar further generalizes this idea to include  $n$  reflecting elements of arbitrary shapes. A similar system, using cones rather than spheres was proposed by Southwell *et al.* [18]. However, in both these systems [12] the projection of the scene produced by the curved mirrors is not from a single point. This turns out to be a disadvantage for many vision techniques (including computational stereo) [10] [13] [20].

Recently, Nayar and Baker [14] derived the complete class of reflecting surfaces that, when imaged by a perspective camera, produce a projection of the scene from a single viewpoint. Based on this general solution, we propose a variety of catadioptric stereo systems that use two or more mirrors and a single lens. Our systems acquire two or more projections of the scene in the same image, where each projection is from a single viewpoint. Mitsumoto *et al.* [9] have previously described a method for recovering depth by acquiring a projection of the scene and its reflection (using a planar mirror) in the same image. Goshtasby and Gruver [2] use a camera pointed at hinged planar mirrors to acquire a pair of images from two viewpoints. Both these are special cases within our general treatment of systems that use multiple planar as well as non-planar mirrors. The catadioptric stereo systems that we propose offer the following advantages over conventional stereo systems that use multiple cameras:

- **Identical System Parameters:** Lens, CCD and digitizer parameters such as blurring, lens distortions, spectral responses, capture synchronization, offset, automatic gain control, pixel size, aspect ratio, etc. are identical for all the views; as if they were taken at the same instant by the same camera-digitizer system.
- **Ease of Calibration:** Since we use only a single

\*This research was supported in parts by the DARPA Image Understanding Program on Video Surveillance and Monitoring and an NSF National Young Investigator Award.

lens, calibration of the system is greatly simplified. This is due to the fact that we need to estimate only one focal length and one center of projection.

- **Wide Field of View:** By use of non-planar reflecting surfaces such as hyperboloids and paraboloids, a wide field of view (while ensuring single viewpoint projection) is easily obtained.
- **Cost:** Lastly, but often most importantly, since a catadioptric stereo system needs only a single camera and a single digitizer, the cost is halved.

## 2 Catadioptric Image Formation

Let us first examine Nayar and Baker's [14] solution of reflecting surfaces that produce a single viewpoint projection. Figure 1 depicts an arbitrary reflecting surface  $S(x, y)$  that induces an effective viewpoint  $v$ . The center of projection (or pinhole) is located at  $p$  and the distance between  $v$  and  $p$  is  $c$ . The coordinate frame is assumed to be located at  $v$ . Since perspective projection is rotationally symmetric around the optical axis  $\hat{z}$ , we consider only a profile  $S(r)$ , where  $r = \sqrt{x^2 + y^2}$ . With this notation in place, the equations that comprise class of mirrors that guarantee a fixed viewpoint are:

$$\left(z - \frac{c}{2}\right)^2 + r^2 \left(1 - \frac{k}{2}\right) = \frac{c^2}{4} \left(\frac{k-2}{k}\right), \quad (1)$$

$$\left(z - \frac{c}{2}\right)^2 + r^2 \left(1 + \frac{c^2}{2k}\right) = \left(\frac{2k + c^2}{4}\right), \quad (2)$$

where,  $k$  is a constant of integration (see [14] for details). Notice that the surfaces described by equations (1) and (2) are conic sections where both  $k$  and  $c$  determine the type of the conic. Nayar and Baker show that the only useful physically realizable surfaces that produce a single viewpoint are planar ( $k = 2$ ), ellipsoidal ( $c > 0, k > 0$ ), hyperboloidal ( $c > 0, k > 2$ ), and paraboloidal ( $c \rightarrow \infty, k \rightarrow \infty$ ).

It is worth mentioning that other researchers have hit upon some of these surfaces. For instance, Rees [17] and Yamazawa *et al.* [20] used a conventional camera pointed at a large hyperboloidal mirror. Nalwa [10] used a pyramidal arrangement of four planar mirrors and four cameras to obtain a single viewpoint wide FOV image mosaic, also at video rates. Nayar used an orthographic camera pointed at a paraboloidal reflecting surface to compute multiple perspective streams from a single parabolic videostream at video rates [13] [16].

## 3 Catadioptric Stereo Systems

We saw that it is possible to setup four kinds catadioptric systems that see the scene from a single viewpoint. In order to obtain depth by triangulation, we

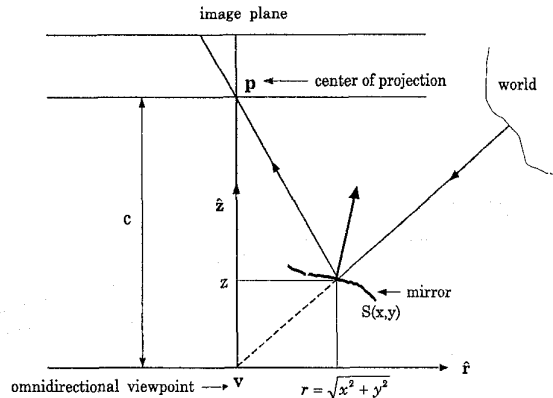


Figure 1: Geometry used to derive the reflecting surface that produces an image of the scene as seen from a fixed viewpoint  $v$  (adapted from [14]).

need two or more projections of the scene as seen from two or more distinct viewpoints. In this section, we shall see that it is possible to setup four kinds of catadioptric *stereo* systems that produce single viewpoint projections. The configurations that we discuss are: a) angled planar mirrors, b) rotated ellipsoidal mirrors, c) rotated hyperboloidal mirrors, d) displaced paraboloidal mirrors (see figure 2). Other systems with combinations of different mirrors are also possible, for instance, planar + hyperboloidal, ellipsoidal + hyperboloidal, etc. We assume that the system is calibrated, which means that camera parameters such as focal length, center of projection, and the location and dimensions of the mirrors are all known. This can be accomplished either by standard techniques such as the 8-point algorithm [4] or by physical measurements.

### 3.1 Angled Planar Mirrors

Figure 2(a) shows a simple stereo system that uses two plane mirrors and a single lens. Such a setup was previously described by Goshtasby and Gruver in [2]. Before we begin our description of this stereo system, let us first gain some insight into catadioptric image formation using a single mirror and lens<sup>1</sup>. It can be shown that acquiring an image of a planar mirror by a pinhole  $p$  at a perpendicular distance  $c/2$  is equivalent to looking at the scene from an effective viewpoint  $v$ , also at a perpendicular distance  $c/2$ , but on the opposite side of  $p$  [14]. This property serves us well, because by placing another mirror at a different orientation (and possibly a different distance  $c'/2$ ), we obtain a new effective viewpoint  $v'$  which is distinct from the viewpoint  $v$ . Hence,

<sup>1</sup>We use the terminology lens, pinhole, and perspective camera interchangeably. A lens has an effective pinhole at it's focus.

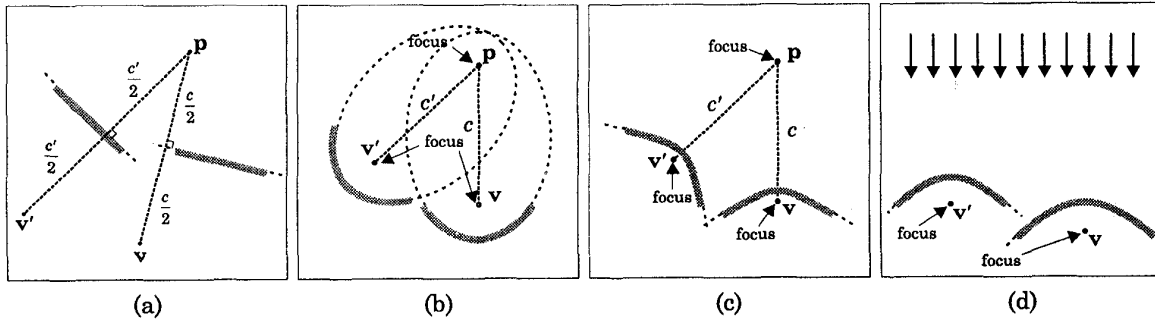


Figure 2: Four different configurations of catadioptric stereo systems are shown. (a) Two planar mirrors at an angle produce two effective viewpoints  $v$  and  $v'$  when imaged by a perspective (pinhole) camera  $p$ . (b) Ellipsoidal mirrors are placed such that one focus of each of the mirrors coincides with the pinhole. The effective viewpoints are located at the other foci. (c) Hyperboloidal mirrors are placed such that the exterior focus of each of the mirrors coincides with the pinhole. The effective viewpoints are located at the other foci. (d) Paraboloidal mirrors placed such that their axes are parallel to each other. When imaged orthographically, the effective viewpoints are located at the interior foci.

by acquiring an image of two or more mirrors at differing orientations from a single lens, it is possible to obtain two or more distinct projections of the scene in the same image.

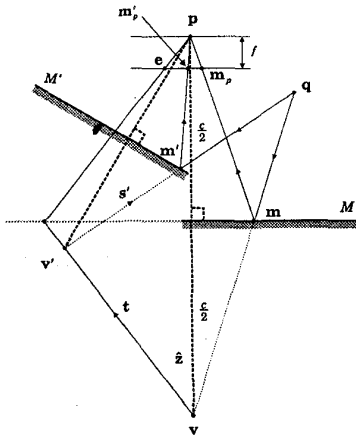


Figure 3: When two planar mirrors are seen from a pinhole  $p$ , they produce two effective viewpoints  $v$  and  $v'$ . The projection of the intersection of the epipolar plane with mirror  $M$  onto the image plane gives the epipolar line for point  $m'_p$ .

Figure 3 shows an arrangement of two planar mirrors and a lens. Let  $p$  be a pinhole at a distance  $c/2$  from the planar mirror  $M$ . Let the image plane be at distance  $f$  from  $p$ . Let  $v$  be the effective viewpoint induced by the mirror  $M$  and pinhole  $p$ . We assume the coordinate system to be conveniently located at  $v$ . Let  $v'(v'_x, v'_y, v'_z)$  be the virtual viewpoint induced by the second mirror  $M'$ . If  $q$  is a scene point, its projections

on the image plane are points  $m_p$  and  $m'_p$ . The rays corresponding to these points intersect the mirrors at  $m$  and  $m'$  respectively.

Given any image point, we can derive an expression for the corresponding epipolar line as follows. The epipolar line corresponding to the image point  $m'_p(x', y')$  is the projection of the line of intersection of the plane passing through points  $v$ ,  $v'$  and  $m'$  and the mirror  $M$ , onto the image plane. As the system is calibrated, the coordinates of  $v'$  are known and the coordinates of point  $m'$  can be computed from  $m'_p$ . Let  $s'(l', m', n')$  be the direction vector of the line joining  $v'$  and  $m'$ . Then, the equation of the plane, which we shall call the *epipolar plane*, can be expressed as:

$$\alpha x + \beta y + \gamma z = 0, \quad (3)$$

where  $\alpha = n'v'_y - m'v'_z$ ,  $\beta = l'v'_z - n'v'_x$ , and  $\gamma = m'v'_x - l'v'_y$ . The surface of the planar mirror  $M$  is given by:

$$z = \frac{c}{2}. \quad (4)$$

Eliminating  $z$  from equations (3) and (4) we get an expression that relates the  $x$  and  $y$  coordinates of any point  $m$  on the line of intersection:

$$2x\alpha + 2y\beta + c\gamma = 0. \quad (5)$$

The perspective projection of a line point  $m(x, y, z)$  onto the image plane to obtain  $m_p(x', y')$  is given by:

$$x' = \frac{fx}{c + \frac{x\alpha + y\beta}{\gamma}}, \quad y' = \frac{fy}{c + \frac{x\alpha + y\beta}{\gamma}}. \quad (6)$$

Now, the equation of the epipolar line is obtained by simply substituting equations (6) in equation (5) and

simplifying:

$$\alpha x' + \beta y' + f\gamma = 0. \quad (7)$$

The epipolar lines generated by equation (7) correspond to the projections of the lines of intersection of the family of planes passing through line  $t$  with the mirror  $M$ . It is easy to see that these lines of intersection converge at the point of intersection of line  $t$  and the mirror  $M$ . The projection of this point onto the image plane gives us the epipolar point  $e(x', y')$ . Thus, to derive the expressions for the coordinates of  $e$ , we proceed as follows. Let  $\hat{t}(\lambda, \mu, \nu)$  be a unit vector in the direction of  $t$ . The equation of a line passing through  $v$  in the direction  $\hat{t}$  is given by:

$$\frac{x}{\lambda} = \frac{y}{\mu} = \frac{z}{\nu}. \quad (8)$$

The perspective projection of this line onto the image plane is:

$$x' = \frac{f\lambda z}{\nu(c-z)}, \quad y' = \frac{f\mu z}{\nu(c-z)}. \quad (9)$$

By substituting in equation (9) the expression for the surface of mirror  $M$  (equation (4)), we immediately get the coordinates of the epipolar point:

$$x' = \lambda \left( \frac{f}{\nu} \right), \quad y' = \mu \left( \frac{f}{\nu} \right). \quad (10)$$

### 3.2 Rotated Ellipsoidal Mirrors

We now look at a more interesting catadioptric stereo system, one that uses a pair of ellipsoidal mirrors and a single lens (see figure 2(b)). Use of such a system gives a wider FOV than can be obtained from a planar mirror system. Figure 4 shows an ellipsoidal mirror  $M$  and a single lens, positioned such that the effective pinhole  $p$  is located precisely at the exterior focus. The mirror reflects light rays passing through the interior focus  $v$  through  $p$  [14]. The image acquired by the lens is a projection of the scene as seen from the viewpoint  $v$ . Another ellipsoidal mirror  $M'$  is placed so that one of its foci lies precisely at  $p$ . Such a mirror will give us another projection, acquired from the viewpoint  $v'$  located at its interior focus. The ellipsoidal mirrors can be of arbitrary sizes provided they all have their distant foci located at  $p$ , which results in a system with the axes of the mirrors rotated with respect to one another.

Unlike the planar mirror system, the epipolar constraints are curves rather than straight lines. The derivation for their expressions, however, proceeds as before. In this case, we wish to find the intersection of the epipolar plane with the surface of the ellipsoid  $M$  and then project this curve of intersection onto the

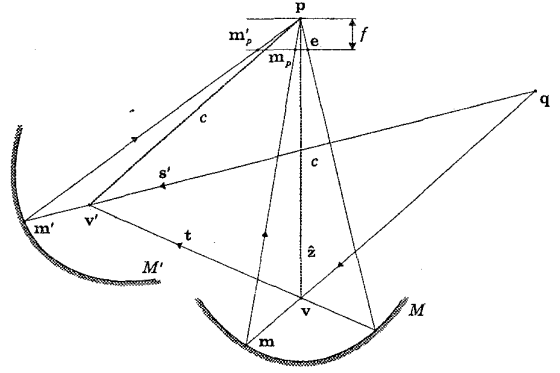


Figure 4: Two ellipsoidal mirrors are precisely positioned such that their distant foci coincide at  $p$ . The viewpoints are located at the closer foci. The projection of the intersection of the epipolar plane with mirror  $M$ , onto the image plane gives the epipolar curve for point  $m'_p$ .

image plane (see figure 4). As before, we assume the coordinate system to be conveniently located at  $v$  and the image plane located at distance  $f$  from pinhole  $p$  perpendicular to the axis  $\hat{z}$  of ellipsoid  $M$ . If  $q$  is a scene point that projects to an image point  $m_p(x', y')$ , the epipolar plane is given by equation (3). Let the surface of the ellipsoid  $M$  be given by:

$$\frac{(z - \frac{c}{2})^2}{a^2} + \frac{x^2 + y^2}{b^2} = 1, \quad (11)$$

where

$$a = \sqrt{\frac{2k + c^2}{4}}, \quad b = \sqrt{\frac{2k}{4}}. \quad (12)$$

First, we eliminate  $z$  from equations (3) and (11) to get the orthographic projection of the curve of intersection of the epipolar plane and the ellipsoid  $M$ . The perspective projection of this curve onto the image plane using equation (6) yields the epipolar curve (see [15] for details):

$$\begin{aligned} & (c^4\gamma^4 + 2kc^2\gamma^4 - k^2\alpha^2\gamma^2)x'^2 \\ & + (c^4\gamma^4 + 2kc^2\gamma^4 - k^2\beta^2\gamma^2)y'^2 \\ & + (2fk^2\alpha\gamma^3 + 2fkc^2\alpha\gamma^3)x' \\ & + (2fk^2\beta\gamma^3 + 2fkc^2\beta\gamma^3)y' \\ & - (2k^2\alpha\beta\gamma^2)x'y' - f^2k^2\gamma^4 = 0. \end{aligned} \quad (13)$$

Observe that equation (13) is a conic section which can be a straight line, circle, ellipse, hyperbola or a parabola depending on the size and position of the ellipsoid  $M'$  and the coordinate of point  $m_p$ .

The expressions for the coordinates of  $e$  are found as in the previous section. We first find the points of intersection of line  $t$  with the ellipsoid  $M$  and then perform

a perspective projection of these points onto the image plane to obtain the coordinates of the epipolar points:

$$\begin{aligned} x' &= \lambda \left( \frac{fk(c\nu \mp \sqrt{c^2 + 2k})}{(1 - \nu^2)c^3 + (2 - \nu^2)ck \pm k\nu\sqrt{c^2 + 2k}} \right), \\ y' &= \mu \left( \frac{fk(c\nu \mp \sqrt{c^2 + 2k})}{(1 - \nu^2)c^3 + (2 - \nu^2)ck \pm k\nu\sqrt{c^2 + 2k}} \right) \end{aligned} \quad (14)$$

### 3.3 Rotated Hyperboloidal Mirrors

A hyperboloidal surface acts much like an ellipsoidal surface, in that it reflects light rays going towards the interior focus  $\mathbf{v}$  through the exterior focus  $\mathbf{p}$ . An image of the mirror acquired by a lens that is positioned precisely such that the effective pinhole lies at  $\mathbf{p}$  is a projection of the scene as seen from the viewpoint  $\mathbf{v}$ . Also like the ellipsoidal system, distinct viewpoints are obtained by placing another hyperboloidal mirror such that its exterior focus is precisely at  $\mathbf{p}$  (see figure 2(c)). Such a system can have an arbitrary number of hyperboloidal mirrors at arbitrary positions provided they all have their exterior foci at the pinhole  $\mathbf{p}$ .

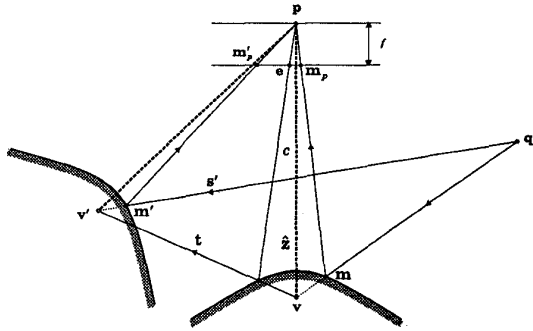


Figure 5: Two hyperboloidal mirrors are precisely positioned such that their exterior foci coincide at  $\mathbf{p}$ . The viewpoints are located at the interior foci. The projection of the intersection of the epipolar plane with mirror  $M$  onto the image plane gives the epipolar curve for point  $\mathbf{m}_p'$ .

To derive expressions of epipolar curves, as before, we find the intersection of the epipolar plane with the surface of the hyperboloid  $M$  and then project this curve of intersection onto the image plane (see figure 5). Let the surface of the hyperboloid  $M$  be given by:

$$\frac{(z - \frac{c}{2})^2}{a^2} - \frac{x^2 + y^2}{b^2} = 1, \quad (15)$$

where

$$a = \frac{c}{2} \sqrt{\frac{k-2}{k}}, \quad b = \frac{c}{2} \sqrt{\frac{2}{k}}. \quad (16)$$

As before, we eliminate  $z$  from equations (3) and (15) and perform a perspective projection of the resulting curve of intersection to obtain the epipolar curve:

$$\begin{aligned} &(-k^2c^4\gamma^4 + 2kc^4\gamma^4 + c^4\alpha^2\gamma^2)x'^2 \\ &+ (-k^2c^4\gamma^4 + 2kc^4\gamma^4 + c^4\beta^2\gamma^2)y'^2 \\ &+ (2fkc^4\alpha\gamma^3 - 2fc^4\alpha\gamma^3)x' \\ &+ (2fkc^4\beta\gamma^3 - 2fc^4\beta\gamma^3)y' \\ &+ (2c^4\alpha\beta\gamma^2)x'y' + f^2c^4\gamma^4 = 0. \end{aligned} \quad (17)$$

As before, the intersection of line  $\mathbf{t}$  with the hyperboloid  $M$  gives us the coordinates of two points, whose perspective projection onto the image plane yields the coordinates of the epipolar points:

$$\begin{aligned} x' &= \lambda \left( \frac{f(\nu \pm \sqrt{1 - \frac{2}{k}})}{(1 - \nu^2)k - (2 - \nu^2) \pm \nu\sqrt{1 - \frac{2}{k}}} \right), \\ y' &= \mu \left( \frac{f(\nu \pm \sqrt{1 - \frac{2}{k}})}{(1 - \nu^2)k - (2 - \nu^2) \pm \nu\sqrt{1 - \frac{2}{k}}} \right) \end{aligned} \quad (18)$$

### 3.4 Displaced Paraboloidal Mirrors

A paraboloidal surface reflects light rays going towards the interior focus  $\mathbf{v}$  such that they are all parallel to its axis. This requires use of an orthographic camera [19] or as a first approximation, a conventional camera kept at a distance from the mirror. This combination of an orthographic camera and a paraboloid produce a projection of the scene from the viewpoint  $\mathbf{v}$  located at the focus. To obtain additional viewpoints, we use additional paraboloidal mirrors which are simply displaced with respect to each other (see figure 2(d)).

The derivation for epipolar curves is now a lot simpler, since there is no need for perspective projection (see figure 6). If the surface of the paraboloid is given by:

$$z = \frac{h^2 - (x^2 + y^2)}{2h}, \quad (19)$$

eliminating  $z$  from equations (3) and (19) and replacing  $x$  by  $x'$  and  $y$  by  $y'$  gives us the epipolar curve:

$$\frac{\gamma}{h}x'^2 + \frac{\gamma}{h}y'^2 - 2\alpha x' - 2\beta y' - h\gamma = 0. \quad (20)$$

Notice that equation (20) is a circle. This implies that straight lines in the scene map to circles<sup>2</sup>, and line segments map to circular arcs. Following the prior procedure, we find the coordinates of the epipolar points by

<sup>2</sup>This observation was first made by Swami Manohar at the Indian Institute of Sciences.

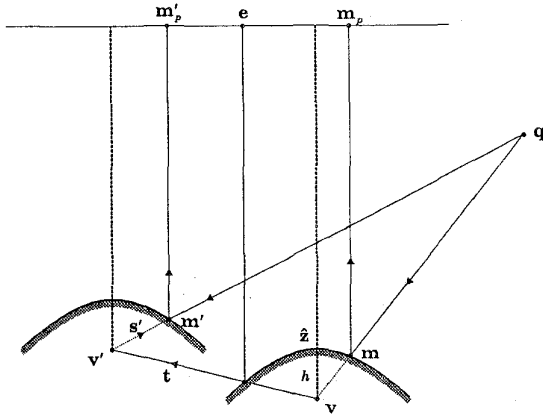


Figure 6: Two paraboloidal mirrors are placed with their axes are parallel to each other. The image of these mirrors is acquired by an orthographic camera. The viewpoints are located at the foci of the respective paraboloids. The projection of the intersection of the epipolar plane with mirror  $M$  onto the image plane gives the epipolar curve for point  $m'_p$ .

intersecting the line  $t$  with the paraboloid  $M$  and projecting the points of intersection onto the image plane to obtain the image coordinates of the epipolar points (details in [15]):

$$x' = \lambda \left( \frac{h}{\nu \pm 1} \right), \quad y' = \mu \left( \frac{h}{\nu \pm 1} \right) \quad (21)$$

#### 4 Field of View

Let us now take a closer look at the field of view (FOV) of catadioptric stereo systems. Figure 7 shows the four systems that we have discussed so far. The thick dotted line is the optical axis of the lens whose effective pinhole is  $p$ . The mirrors induce effective viewpoints  $v$  and  $v'$ . The thin dotted lines correspond to the field of view of each mirror and lens (camera) system taken individually. This also means that the camera will see itself and will not see the scene behind it. To keep the illustration clear, we have not shown this self occlusion. The gray areas correspond to regions of mutual occlusion due to one mirror blocking the other's view. The FOV of the complete system is the region (marked in bold) common to the individual FOVs minus the regions of mutual and self occlusion. We formalize this as follows.

Let  $\mathcal{V}_1 \in \mathbf{R}^3$  represent the set of all scene points visible from the viewpoint  $v$  of a single lens and mirror catadioptric system. Let  $\mathcal{C}_1 \in \mathbf{R}^3$  represent the set of all scene points occluded by the camera as seen from

the viewpoint  $v$ . Then, the FOV  $\mathcal{F}$  of this system is simply:

$$\mathcal{F} = \mathcal{V}_1 - \mathcal{C}_1. \quad (22)$$

Let us now consider a catadioptric stereo system with a pair of mirrors and a single lens. In this case, we need to consider  $\mathcal{M}_{2,1}, \mathcal{M}_{1,2} \in \mathbf{R}^3$ , the sets of scene points occluded by mirrors  $M'$  and  $M$  from viewpoints  $v$  and  $v'$ , respectively. If  $\mathcal{C}_1$  and  $\mathcal{C}_2$  are the regions of self occlusion of the cameras from the viewpoints  $v$  and  $v'$ , respectively, then the FOV of the system can be written as:

$$\mathcal{F} = (\mathcal{V}_1 - \mathcal{C}_1 - \mathcal{M}_{2,1}) \cap (\mathcal{V}_2 - \mathcal{C}_2 - \mathcal{M}_{1,2}). \quad (23)$$

Generalizing this to  $k$  mirrors, we get:

$$\mathcal{F} = \bigcap_{i=1}^k \left( \mathcal{V}_i - \mathcal{C}_i - \bigcup_{j=1}^k \mathcal{M}_{j,i} \right), \quad \mathcal{M}_{i,i} = \emptyset. \quad (24)$$

Equations (23) and (24) are in general non-trivial to evaluate analytically. A numerical solution is possible using visibility estimation techniques such as [1].

#### 5 Experiments

The goal of our first experiment was to obtain a dense depth map using a CCD camera pointed at two planar mirrors. The camera and mirrors were freely positioned to obtain two views (in the same image) of a candy box, shown in figure 8(a). A black background was used to avoid segmentation related issues. The 8-point algorithm of Hartley [4] was used to compute the fundamental matrix for the two views of the candy box after manually corresponding 20 features. Figure 8(a) shows epipolar lines corresponding to few randomly selected features marked in the view on the left. Estimation of correspondence by normalized correlation and back-matching followed by 3x3 median filtering gave us disparity along epipolar lines. Next, the factorization technique of Hartley [3] was used to obtain the focal length and the rotation and translation of coordinate frames centered at the effective viewpoints corresponding to the two views. This enabled us to compute the 3-D structure of the candy box. A gray-coded image of depth obtained for every pixel in the left view is shown figure 8(b). Figure 8(c) shows a texture mapped rendering of a novel view of the candy box obtained from a virtual camera situated a little to the left, above and closer (and hence the enhanced perspective effect) to our original camera.

In the second experiment, our goal was to demonstrate that depth can be computed using curved mirrors. We used two paraboloidal mirrors and a 35mm SLR camera, since this setup gives us the most freedom

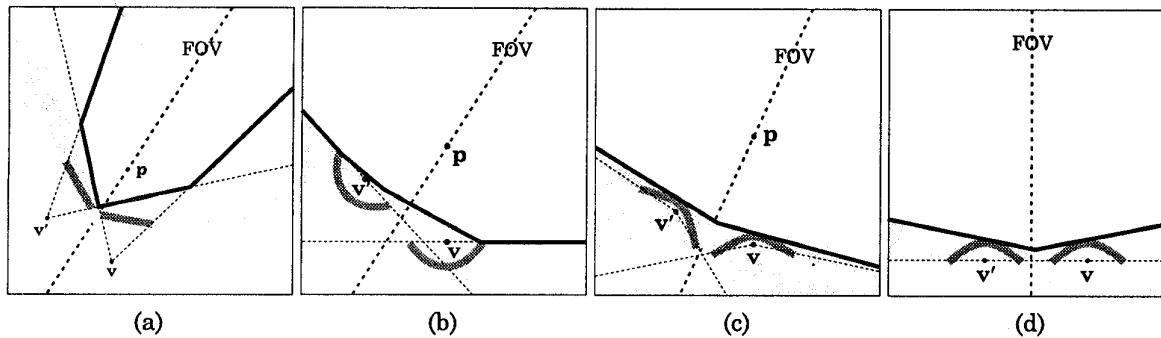


Figure 7: Four stereo systems are illustrated: (a) planar, (b) ellipsoidal, (c) hyperboloidal, and (d) paraboloidal. In each case, the FOV from each effective viewpoint is shown by thin dotted lines. The position of the pinhole camera is marked by  $p$ . The thick dotted line indicates the optical axis of the camera. The areas marked faint gray are regions of mutual occlusion. For each system, the FOV is determined by intersecting the individual FOVs from each effective viewpoint and subtracting the areas of mutual occlusion. The resulting FOV is marked in each case by the solid thick lines.

and convenience in positioning the mirrors and the camera. The mirrors were fixed to a base kept on the floor. The camera was suspended 6 feet above using a tripod. At this distance, zooming-in close to the mirrors gave us the desired orthographic projection. Figure 8(d) shows an image acquired by this setup. It was scanned in at a resolution of 1068x750 using a Nikon slide scanner. The objects used in our experiment were a box and a cylinder placed about  $180^\circ$  apart. Calibration was performed by noting the pixel coordinates of the centers of the paraboloidal mirrors and measuring their radi  $h$ , also in pixel units. Notice in figure 8(d) that the centers etched on the paraboloidal mirrors are visible as small white dots. Next, we used equation (20) to compute epipolar curves. Epipolar curves corresponding to sample scene features are illustrated in figure 8(d). Before estimating correspondence, we cut out the objects manually from the background. Normalized correlation using a  $9 \times 9$  window was performed to obtain disparity for each point on the lower right paraboloidal image. This allowed us to triangulate and compute depth for each point. A gray-coded depth image thus obtained is shown in figure 8(e). The experiment thus demonstrates that it is indeed practical to obtain wide FOV depth images by use of paraboloidal mirrors and a single camera. In the future, we plan to refine our current implementation and develop compact and easy to use systems in various configurations that utilize the four types of reflecting surfaces that we discussed.

## References

- [1] S. Abrams, P. K. Allen, and K. A. Tarabanis. Dynamic sensor planning. In *Proceedings of IEEE International Conference on Robotics and Automation*, Atlanta, May 1993.
- [2] A. Goshtasby and W. A. Gruver. Design of a single-lens stereo camera system. *Pattern Recognition*, 26(6):923–937, 1993.
- [3] R. I. Hartley. Estimation of relative camera positions for uncalibrated cameras. In *Proceedings of European Conference on Computer Vision (ECCV '92)*, pages 579–587, 1992.
- [4] R. I. Hartley. In defence of the 8-point algorithm. In *Proceedings of Fifth International Conference on Computer Vision (ICCV '95)*, pages 1064–1070, Cambridge, Massachusetts, June 1995.
- [5] E. Hecht and A. Zajac. *Optics*. Addison Wesley, Reading, Massachusetts, 1974.
- [6] H. Ishiguro, M. Yamamoto, and S. Tsuji. Omnidirectional stereo. *IEEE Transactions on Pattern Analysis and Machine Intelligence (PAMI)*, (14):257–262, 1992.
- [7] S. B. Kang and R. Szeliski. 3-d scene data recovery using omnidirectional multibaseline stereo. In *Proceedings of IEEE Conference on Computer Vision and Pattern Recognition (CVPR' 96)*, pages 364–370, San Francisco, June 1996.
- [8] L. McMillan and G. Bishop. Plenoptic modeling: An image-based rendering system. In *Computer Graphics (SIGGRAPH 95)*, pages 39–46, Los Angeles, August 1995.
- [9] H. Mitsumoto, S. Tamura, K. Okazaki, N. Kajimi, and Y. Fukui. 3d reconstruction using mirror images based on a plane symmetry recovery method. *IEEE Transactions on Pattern Analysis and Machine Intelligence (PAMI)*, 14(9):941–945, 1992.
- [10] V. Nalwa. A true omnidirectional viewer. Technical report, Bell Laboratories, Holmdel, NJ 07733, February 1996.
- [11] S. K. Nayar. Sphereo: Recovering depth using a single camera and two specular spheres. In *Proceedings*

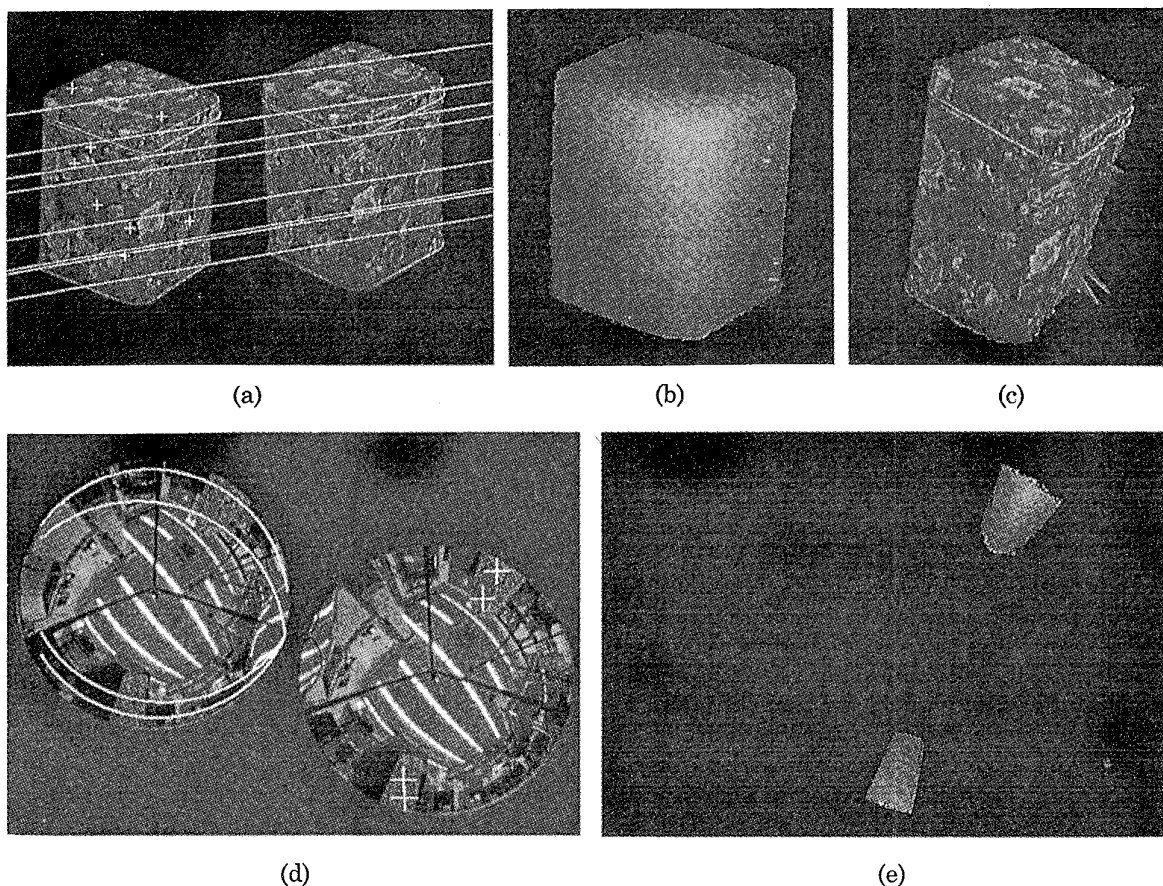


Figure 8: In the first experiment, a camera was pointed at two planar mirrors to obtain (a) two views of a candy box in the same image. Epipolar lines corresponding to features marked by crosses are also shown. The computed depth is illustrated as (b) a gray-coded depth image and (d) a texture mapped novel image from a viewpoint that is closer, to the left, and above the original viewpoint. In the second experiment, a camera was suspended above two parabolic mirrors. (d) Epipolar curves corresponding to sample features are shown. (e) A gray coded depth image for the two objects in the lower right parabola is shown.

*of SPIE: Optics, Illumination, and Image Sensing for Machine Vision II*, November 1988.

[12] S. K. Nayar. Robotic vision system, January 1990. United States Patent 4,893,183. Filed August 11, 1988.

[13] S. K. Nayar. Omnidirectional video camera. In *Proceedings of DARPA Image Understanding Workshop*, New Orleans, May 1997.

[14] S. K. Nayar and S. Baker. Catadioptric image formation. In *Proceedings of DARPA Image Understanding Workshop*, New Orleans, May 1997.

[15] S. A. Nene and S. K. Nayar. Stereo with mirrors. Technical report, Department of Computer Science, Columbia University, September 1997.

[16] V. N. Peri and S. K. Nayar. Generation of perspective and panoramic video from omnidirectional video. In *Proceedings of DARPA Image Understanding Workshop*, New Orleans, May 1997.

[17] D. W. Rees. Panoramic television viewing system, April 1970. United States Patent 3,505,465.

[18] D. Southwell, A. Basu, M. Fiala, and J. Reyda. Panoramic stereo. In *Proceedings of International Conference on Pattern Recognition (ICPR '96)*, Vienna, Austria, August 1996.

[19] M. Watanabe and S. K. Nayar. Telecentric optics for computational vision. In *Proceedings of European Conference on Computer Vision (ECCV '96)*, April 1996.

[20] K. Yamazawa, Y. Yagi, and M. Yachida. Omnidirectional imaging with hyperboloidal projection. In *Proceedings of International Conference on Robots and Systems (IROS)*, 1993.